

Instability of Adsorbed Films of 1-Dodecanol and its Mixture with Sodium Dodecyl Sulfate at the Air/Water Interface

Chika Akabane, Ken-ichi Iimura, Shinji Yamada¹, Tomoya Uruga², Hajime Tanida², Hidenori Toyokawa², Yasuko Terada², and Gerald Brezesinski³

Utsunomiya University, 7-1-2 Yoto, Utsunomiya 321-8585, Japan

¹ Kao Corporation, 2-1-3 Bunka, Sumida-ku, Tokyo 131-8501, Japan

² JASRI (SPring-8), 1-1-1 Koto, Sayo, Hyogo, Japan

³ Max-Planck Institute of Colloids and Interfaces, D-14476 Potsdam, Germany

Fax: 81-28-689-6179, e-mail: emlak@cc.utsunomiya-u.ac.jp

Properties and structures of adsorbed films on mixed aqueous solutions of sodium dodecyl sulfate (SDS) and a trace amount of 1-dodecanol (DD) were investigated by film balance experiments, a Brewster angle microscopy (BAM), and a quick X-ray reflectometry (q-XR) at 20 °C. Pouring the aqueous solutions of the surfactants into a trough, the surface pressure first increased up to certain maximum values due to adsorption of the surfactants at the air/solution interface, but after a while it started to decrease probably due to evaporation of DD. BAM observation showed formation of holes of fluid phase in homogeneous condensed-phase monolayers in the course of surface pressure decrease. The q-XR technique was applied to the adsorbed films at the beginning stage of destabilization in order to characterize the film structures at the molecular level.

Key words: adsorbed film, sodium dodecyl sulfate, dodecanol, X-ray reflectivity, air/water interface

1. INTRODUCTION

Sodium dodecyl sulfate (SDS) is one of important anionic surfactants in detergent and cosmetic industries. Adsorption and phase behavior of SDS at the air/water interface have been studied extensively. A common insight gained from the studies is that interfacial properties of the SDS solution are drastically affected by a trace amount of impurities. Usually, commercially available pure SDS contains 0.1 – 1 % dodecanol (DD). DD is highly surface-active, and even a small amount of DD gives significant changes in surface tension [1,2], surface viscosity [3], and foam stability [4].

Recent advances in surface analytic techniques allow us to investigate the air/water interface in detail. For instance, coadsorption of SDS and medium-chain alcohols at the air/solution interface was studied by equilibrium and dynamic surface pressure experiments, BAM, and a grazing-incidence X-ray diffraction (GIXD) by Vollhardt *et al* [5-8]. In their experimental conditions, a highly purified SDS formed only a fluid-like phase with no phase transition in a surface pressure (π) – adsorption time (t) curve, whereas the films on the surfaces of the pure DD solution and on the mixed solutions of SDS with a trace amount of DD underwent the first-order phase transition from an expanded to a condensed phase. BAM observation showed consequent growth of condensed-phase domains during the phase transition: fractal-like shaped domains emerged at the beginning stage of the phase transition and finally coalesced to form a homogeneous monolayer. The molecular packing structure at the interface was evaluated by GIXD. In the films on the SDS/DD solutions, the surfactant molecules are packed in an untilted hexagonal lattice with dimensions almost corre-

sponding to those obtained for the pure DD monolayer. These observations indicate that DD dominates the two-dimensional properties and structures in the mixed films even though DD is a further minor component in the mixed solutions.

Quantitative information on surfactant composition was provided for the adsorbed films on the surface of a 6 mM solution containing of 99.9% SDS and 0.1 % DD (w/w) using sum-frequency spectroscopy and ellipsometry [9]. Depending on temperature of the solution surface, the monolayer state and composition were changed. At temperatures below the two-dimensional phase transition temperature, T_m , the film was conformationally ordered with a surface coverage comparable to that of the pure DD monolayer at the same temperatures. For this condition, the contents of DD and SDS in the film, estimated from SFS data, were 49 % and 51 % respectively. On the other hand, at higher temperatures than T_m , the film was more disordered than the corresponding liquid phase of pure DD, and was composed of 39% DD and 61% SDS.

In this paper, we report instability of adsorbed films on the surfaces of pure DD and mixed SDS/DD solutions. Despite of a large number of literatures concerning the SDS/DD films at the surfactant solutions/air interface, it is hard to find papers describing the instability of the films. Here, the interfacial properties and structures are investigated as a function of time by the film balance, BAM, and q-XR at 20 °C.

2. EXPERIMENTAL SECTION

SDS used in this study originally contains 0.10 wt% DD. Hence we take this amount into account for calculation of solution concentration beforehand. The

ultrapure water was used for all experiments.

A total concentration of SDS and DD in their mixed solutions was 2.5 mM, and the content of DD was changed from 0.15 to 15 mol%. Hereafter, the mixed solutions are named by the total surfactant concentration with the DD mole percent in the solutions; for example, a 2.5 mM SDS/DD solution containing 1.0 mol% DD is referred to as "2.5 mM SDS/1.0 mol% DD". The concentration of a pure DD solution was 25 μM .

Surface pressure (π) was measured by the Wilhelmy method with a Langmuir film balance. A defined volume of surfactant solution was poured into a Teflon trough directly from a glass flask, and this time was set to $t = 0$. The same volume of ultrapure water was used to give $\pi = 0 \text{ mNm}^{-1}$. BAM observation was performed simultaneously with π - t experiments using EP³-BAM (Nanofilm Technologie GmbH, Gottingen, Germany). The laser used was a solid-state laser (wavelength of 532 nm, 50 mW) and the resolution of image was about 2 μm .

Specular XR experiments were performed with a liquid surface reflectometer recently developed at the undulator beamline BL37XU in SPring-8 (Hyogo, Japan) [11]. A monochromatic synchrotron X-ray beam with the wavelength of $\lambda = 0.827 \text{ \AA}$ ($\sim 15 \text{ keV}$) was deflected downwards onto the solution surface by tilting a silicon (111) crystal. The reflected beam was detected by a two-dimensional hybrid pixel array detector, PILATUS (487 \times 195 pixels with 172 μm / pixels) [12] as a function of the incident angle, α_i . The α_i was varied in the range of 0.005 – 2.95°, corresponding to q_z of 0.001 – 0.78 \AA^{-1} where $q_z = (4\pi/\lambda)\sin\alpha_i$. The advantage of this XR system is "quick measurement" by the use of PILATUS and the simultaneous multi-axes control systems. It took only about 4.5 min to obtain one XR profile shown later, which is much shorter compared with normal XR measurements with a scintillation detector. The fitting analysis was made using the Parratt program (Hahn-Meitner Institute, Berlin, Germany).

All experiments of π - t measurements, BAM, and q-XR were performed at 20 °C.

3. RESULTS AND DISCUSSION

3.1 Surface Property and Morphology

Fig. 1 shows a π - t curve for the 25 μM DD solution. The surface pressure once increases after pouring the solution into the trough, and then decreases over 16 hr. In the inset, one can see a first-order phase transition from an expanded to a condensed phase at about 20 mNm^{-1} . We indeed observed very rapid growth of elongated, fingering-shaped domains of condensed-phase during the phase transition period with BAM, but the images could not be captured since the growing domains vigorously flowed on the solution surface. Around the maximum of surface pressure, the solution surface seemed to be almost covered with a homogeneous condensed-phase film. At the beginning of the surface pressure decrease, we could not recognize any morphological change. However development of holes could be seen when the surface pressure decreased below approximately 20 mNm^{-1} , as shown in Fig. 2. An area occupied by the holes increases with time, accompanying with gradual lowering of surface pressure.

Apparently, the holes belong to the expanded phase, so the plateau below 20 mNm^{-1} should correspond to the reversed phase-transition region from the condensed to the expanded phase. After a break point at about 4 hr in the π - t curve, the surface looked homogeneous with the expanded phase.

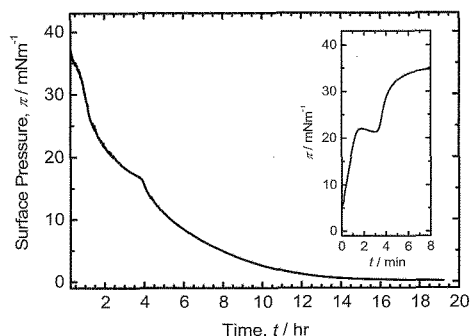


Fig. 1 A π - t plot for the 25 μM DD solution. The inset shows the surface pressure change at the early stage of

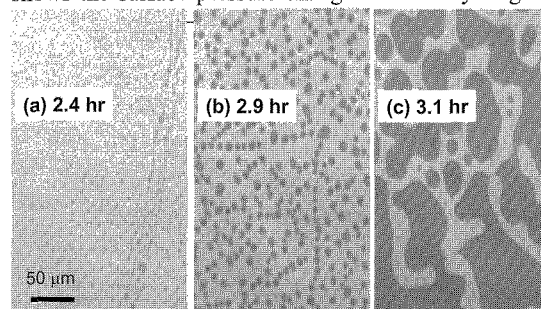


Fig. 2 BAM images for the 25 μM DD solution surface, observed at $t =$ (a) 2.4 hr, (b) 2.9 hr, (c) 3.1 hr in the π - t measurement shown in Fig. 1.

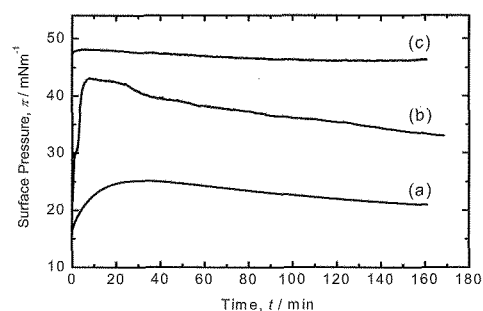


Fig. 3 π - t plots for solutions of (a) 2.5 mM SDS/0.30 mol% DD, (b) 2.5 mM SDS/1.15 mol% DD, (c) 2.5 mM SDS/15.1 mol% DD.

Evaporation of DD from the air/water interface has been reported [13]. Consequently we think that the surface pressure decrease mentioned above would also be caused by evaporation of DD from the air/water interface with time. The surface pressure instability is observed for DD/SDS mixed solutions, too (Fig. 3). One will see that the maximum surface pressure becomes higher with the increase of DD content in the solutions. According to BAM and GIXD (results are not shown

here) [14], the state of adsorbed film at the maximum surface pressure is the fluid phase for the 2.5 mM SDS/0.30 mol% DD solution, and the solid phase for the 2.5 mM SDS/1.15 mol% and 15.1 mol% solutions. The decreasing rate of surface pressure is also very dependent on the mixing ratio. The rate seems to be quite slow for the 2.5 mM SDS/15.1 mol% DD solution, compared with other two solutions.

3.2 X-ray Reflectivity (XR)

XR profiles are shown for the adsorbed films on the 25 μ M DD solution in Fig.4, the 2.5 mM SDS/1.15 mol% DD solution in Fig.5, and the 2.5 mM SDS/14.1 mol% DD solution in Fig.6. The measurement was repeated every 5 min, but only selected profiles are shown in the figures. It should be noted that because the observed data below $R = \text{ca. } 5 \times 10^{-9}$ ($q_z > 0.6$) are rather scattered, we discuss the XR profiles above this intensity.

For the 25 μ M DD solution (Fig.4), the XR measurement was performed until $t = 40$ min at which the surface pressure already started to decrease. However, the profiles at $t = 10$ min and at 40 min almost perfectly coincide with each other. The similar conclusion could be derived for the 2.5 mM SDS/1.15 mol% DD solution (Fig.5), in which the last measurement started at $t = 43$ min and no perceptible difference could be seen between the profiles of $t = 13$ min and $t = 43$ min. These observations indicate that some physical events, which would originate from evaporation of DD, should occur at the interface to reduce the surface pressure, but do not give influence to the XR profiles within our measurement time.

For the 2.5 mM SDS/14.1 mol% DD solution, the profiles coincide with each other till $t = 16$ min. However, remarkable, sudden changes are observed for the profile of $t = 21$ min, in which the reflectivity drops rapidly and the critical angle α_c shifts to a higher value. After this time, the shift of α_c continuously proceeded with time, and the reflectivity profile had never returned to the initial ones. These changes indicate that the interface structure became too complicated to be applied by the usual X-ray reflectivity technique. We assume that the changes might be related to deposition of unsolved DD at the interface. The solubility of DD in water was reported to 25 μ M [15], which is much less than the concentration of DD in the 2.5 mM SDS/14.1 mol% DD solution. At present, we expect the deposited DD phase coexists with the monolayer of DD/SDS on the solution surface or is beneath the monolayer. Tajima *et al.* studied adsorption of SDS/DD at the solution/air interface by the radiotracer method [16]. They observed

that the total concentration of adsorbed surfactants exceeds the amount expected for the close-packed monolayer adsorption. The change observed in our XR profiles would also reflect existence of the excess amount of DD at the interface. We are now trying to identify the structure by BAM and FT-IR. If the deposited DD domains disperse on the solution surface with distance of several tens micrometers, a micro-beam X-ray technique may also give useful information on the interface structure.

The fitting analyses were performed for XR profiles stably obtained ($t = 40$ min for the 25 μ M DD solution, $t = 43$ min for the 2.5 mM SDS/1.15 mol% DD solution, and $t = 6$ min for the 2.5 mM SDS/14.1 mol% DD). The fitted parameters of the length l , the electron density

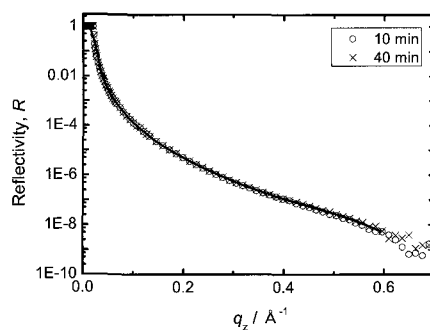


Fig. 4 XR profiles for the 25 μ M DD solution, obtained by starting the measurements at $t = 10$ min and 40 min after pouring the solution into the trough. The full line corresponds to the fitted one for the profile of $t = 40$ min.

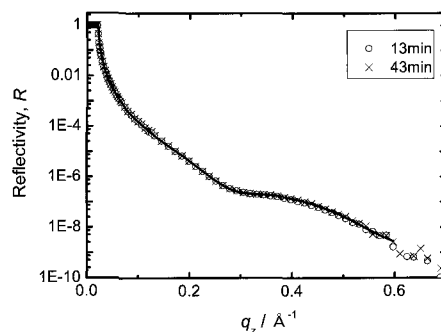


Fig. 5 XR profiles for the 2.5 mM SDS/1.15 mol% DD solution, obtained by starting the measurements at $t = 13$ min and 43 min after pouring the solution into the trough. The full line corresponds to the fitted one for the profile of $t = 43$ min.

Table I The fitted parameters for the adsorbed films on the solutions of 25 μ M DD ($t = 40$ min), 2.5 mM SDS/1.15 mol% DD ($t = 43$ min), and 2.5 mM SDS/14.1 mol% DD ($t = 6$ min).

solution	tail			head			water
	l_t [Å]	ρ_t [Å ⁻³]	σ_t [Å]	l_h [Å]	ρ_h [Å ⁻³]	σ_h [Å]	σ_w [Å]
25 μ M DD	15.1	0.311	2.9	0.97	0.446	3.6	3.1
2.5 mM SDS/ 1.15 mol% DD	15.1	0.308	3.3	2.00	0.559	3.7	3.9
2.5 mM SDS/ 14.13 mol% DD	15.2	0.309	3.6	1.31	0.523	3.7	3.7

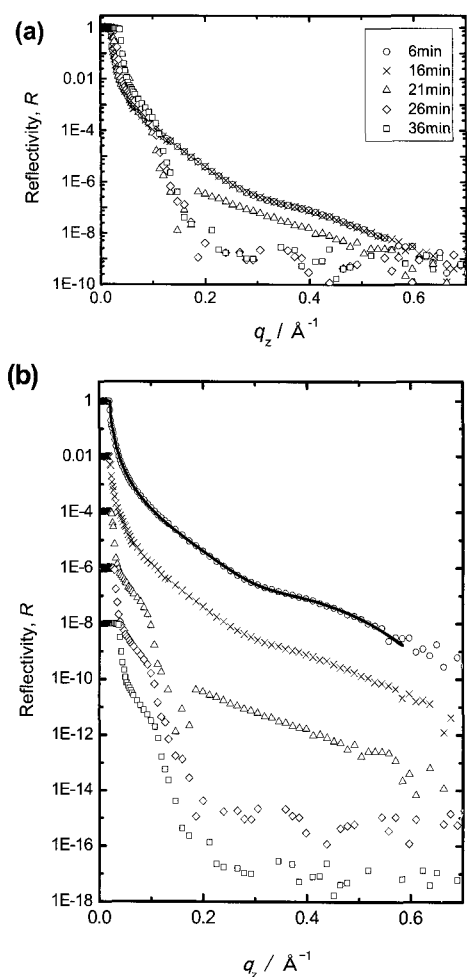


Fig. 6 XR profiles for the 2.5 mM SDS/14.1 mol% DD solution. The reflectivity scales are shifted by 10^{-2} unit between profiles. The full line in (b) corresponds to the fitted one for the profile of $t = 6$ min.

ρ , and the roughness σ are summarized in Table I. The number of electrons N_e for the hydrophobic tail is estimated by $A \times l_t \times \rho_t$, where A is the molecular area. Adopting $A = 21 \text{ \AA}^2$ based on GIXD data (not shown), the fitted parameters give N_e s of 98.4, 97.5, and 98.4 for the adsorbed films on the 25 μM DD, 2.5 mM SDS/1.15 mol% DD, and 2.5 mM SDS/14.13 mol% DD solutions, respectively. These numbers are slightly larger than the ideal one $N_e = 97$ for $(\text{CH}_2)_{11}\text{CH}_3$ chain, but are enough acceptable. The length of $l_t = 15.1 - 15.2 \text{ \AA}$ is almost equivalent to that expected for the fully stretched C12 chain with all-trans conformation (15.4 \AA) [17]. The number of electron in the head group (i.e. hydroxyl group) of DD is estimated to be 9.1 using $A = 21 \text{ \AA}^2$, $l_h = 0.97 \text{ \AA}$, and $\rho_h = 0.446$, which in good agreement with the ideal one. Finally, if SDS and DD are mixed in the adsorbed films with the mixing ratios corresponding to those in the solutions, the ρ_h for the 2.5 mM SDS/1.15 mol% DD solution and 2.5 mM SDS/14.13 mol% DD solution would be approximately 1.9 \AA^{-3} . The ρ_h s obtained for these films by the fitting analyses clearly deny this assumption, indicating a much larger number of the DD molecules adsorb on the surface of the SDS/DD solutions.

4. SUMMARY

The properties and structures of adsorbed films on the surfaces of 25 μM DD solution and 2.5 mM SDS/DD solutions were studied at 20 $^\circ\text{C}$. We clearly show the surface pressure instability of the adsorbed films on the 25 μM DD and 2.5 mM SDS/1.15 mol% DD solutions, which might be induced by evaporation of DD from the interface. On the other hand, the surface pressure for the 2.5 mM SDS/14.1 mol% DD solution is considerably stable compared with the pure DD and lower DD content solutions. The film structure for this solution is expected to be composed of the monolayer of DD/SDS with a DD phase deposited due to the solubility limit.

The composition in the adsorbed films is discussed based on the q-XR data. It is shown that the adsorbed films contain a larger number of DD than expected from the mixing ratios in the solutions. Further studies are now in progress to clarify unique properties of the DD and SDS/DD film systems in detail.

Acknowledgement

The XR experiments were performed at SPring-8 with the approval of Japan Synchrotron Radiation Research Institute (JASRI) (2007B1510).

References and Note

- [1] K. J. Mysels, *Langmuir*, **2**, 423-438 (1986)
- [2] D. Vollhardt, and G. Czichocki, *Langmuir*, **2**, 317-322 (1990)
- [3] A. M. Poskanzer, and F. C. Goodrich, *J. Phys. Chem.*, **79**, 2122-2126 (1975).
- [4] G. D. Miles, L. Shedlovsky, and J. Ross, *J. Phys. Chem.*, **45**, 93-107 (1945)
- [5] D. Vollhardt, G. Brezesinski, S. Siegel, and G. Emrich, *J. Phys. Chem. B.* **105**, 12061-12067 (2001).
- [6] D. Vollhardt and G. Emrich, *Colloid and Surfaces, A*, **161**, 173-182 (2000)
- [7] V. B. Fainerman, D. Vollhardt, and G. Emrich, *J. Phys. Chem. B.* **105**, 4324-4330 (2001).
- [8] D. Vollhardt, V. B. Fainerman, and G. Emrich, *J. Phys. Chem. B.* **104**, 8536-8543 (2000).
- [9] B. D. Casson and C. D. Bain, *J. Phys. Chem. B.* **102**, 7434-7441 (1998).
- [10] T. Riste and D. Sherrington J., Ed., *Phase Transitions in Soft Condensed Matter.*, Plenum Press, p.113-138 (1989).
- [11] Y. F. Yano, T. Uruga, H. Tanida, H. Toyokawa, Y. Terada, M. Takagak, *J. Phys.: Conference Series*, **83**, 012024-1-6 (2007).
- [12] Ch. Broennimann, E. F. Eikenberry, B. Henrich, R. Horisberger, G. Huelsen, E. Pohl, B. Schmitt, C. Schulze-Briese, M. Suzuki, T. Tomizaki, H. Toyokawa, A. Wagner, *J. Synchrotron Rad.*, **13**, 120 (2006).
- [13] G. L. Gaines, Jr., Ed., *Insoluble Monolayers at Liquid-Gas Interface*, Interscience Publishers, p.208 (1966).
- [14] GIXD experiments were performed using the liquid surface diffractometer on the undulator beamline BW1 in HASYLAB at DESY (Hamburg, Germany).
- [15] G. L. Amidon, S. H. Yalkowsky, S. Leung, *J. Pharm. Sci.*, **63**, 1858-1866 (1974).
- [16] K. Tajima, M. Muramatsu, T. Sasaki, *Bull. Chem. Soc. Jpn.*, **42**, 2471-2475 (1969).
- [17] C. A. Helm, H. Moehwald, K. Kjeaar, J. Als-Nielsen, *Europhys. Lett.*, **4**, 697-703 (1987).